2

Naval Ocean Research and Development Activity
Stennis Space Center, Mississippi 39529-5004

NORDA Technical Note 427
September 1990

Converting Digital Passive Microwave Radiances to Kelvin Units of Brightness Temperatures

L. D. Farmer
D. T. Eppler
A. W. Lohanick
Oceanography Division
Ocean Science Directorate

DISCLAIMER NOTICE

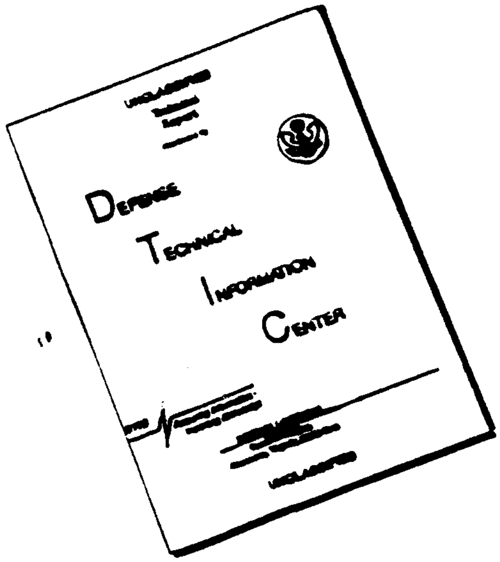

THIS DOCUMENT IS BEST QUALITY AVAILABLE. THE COPY FURNISHED TO DTIC CONTAINED A SIGNIFICANT NUMBER OF PAGES WHICH DO NOT REPRODUCE LEGIBLY.

ABSTRACT

The K_a-band Radiometric Mapping System (KRMS) has been utilized since 1983 to collect digital records of microwave radiances. This report details methods for converting these digital radiances to appropriate units of brightness temperature.

ACKNOWLEDGMENTS

The work reported here was supported by NOARL (formerly NORDA) Program Element 61153N (Herbert Eppert, Program Manager), and by the NASA Oceanic Processes Branch through the SSM/I Validation Program (Robert Thomas, Program Manager).

CONTENTS

ILLUSTRATIONS

Figure

TABLE

Table

Converting Digital Passive Microwave Radiances to Kelvin Units of Brightness Temperatures

L. DENNIS FARMER, DUANE T. EPPLER AND ALAN W. LOHANICK

INTRODUCTION

NOARL, in conjunction with the Naval Weapons Center (NWC) at China Lake, California, has been collecting passive microwave imagery with the K_a-band Radiometric Mapping System (KRMS) since 1983. With the exception of the 1983 data, none of these data have been converted to brightness temperatures. The KRMS is not a calibrated system; however, the 1983 data were converted to brightness temperatures using the engineering method described in NORDA Report 51 (Eppler et al. 1984), which required measuring the gains and losses within the system and then scaling the resultant radiances to surface-measured values for open water and first-year ice.

The system has a measured reference load that may be related to brightness temperature using the conversion graph produced at NWC (Fig. 1). This provides a warm reference point. The cool reference point (or tie-point) used is an assumed brightness temperature for open water at nadir, 135 kelvins (K). Another possible method is to use a local ambient temperature at the surface adjusted for the highest anticipated emissivity for sea ice (0.94) and use this as the warm tie-point.

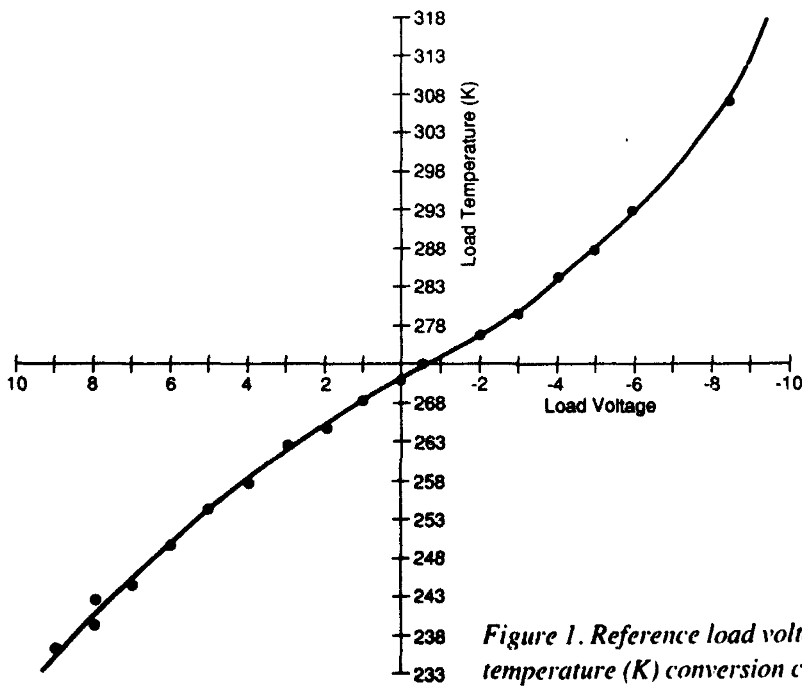

Figure 1. Reference load voltage to temperature (K) conversion chart.

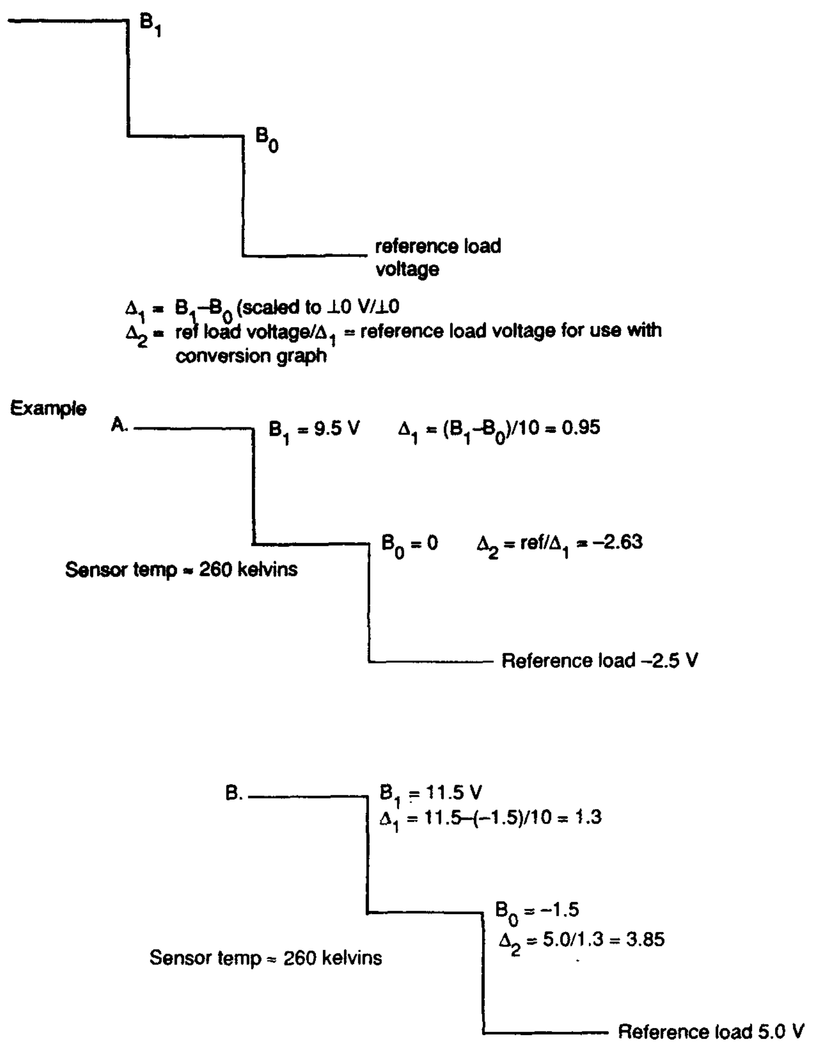

Figure 2. Determining proper reference load voltage for use with graph shown in Figure 1.

BACKGROUND

Data from three KRMS missions were used to evaluate the conversion procedures: 1) data from a NORDA field experiment conducted in March 1983 (Eppler et al. 1984); 2) data from the GEOSAT/LIMEX experiments conducted in March 1987 (Farmer et al. 1989); and 3) data from the March 1988 SSM/I calibration/validation experiment (Farmer et al. 1989). The conversion procedures presented make several assumptions. First, we assume that the lowest apparent brightness temperature in a scene is greater than or equal to that for smooth open water at nadir, approximately 135 K (Hollinger 1973, Hollinger and Lo 1983). This open water value is a surface measurement of a calm sea at nadir and does not take into account atmospheric effects (the distance between the sensor and the surface is known, but the atmospheric contributions to the signal are ignored) or the effect of surface roughness. Open water represents, radiometrically, the coolest surface observed in KRMS scenes of sea ice

(Eppler et al. 1986). Since

$$T_b = E \times T_t \quad (1)$$

where T_b is the brightness temperature, E the emissivity and T_t the physical temperature, we can relate T_b to the physical temperature of a surface. If we assume that the emissivity of a calm sea is 0.50 at nadir, and that the thermal temperature of exposed arctic seawater is at its freezing point (−1.8° C or 271.36 K), then, from eq 1, the brightness temperature (T_b) of open water measured at the sea surface is 136.68 K. Hollinger (1973, 1983) and Stogryn (1971) predict similar values. Second, we assume that the highest brightness temperature can be estimated using either a known surface temperature (ambient) or by measuring the reference load voltage and computing the equivalent brightness temperature from the NWC graph (Fig. 1). If these assumptions hold, then the range of digital radiance values present in a KRMS data set can be linearly scaled to brightness temperatures that fall within this range. Our approach is to define tie-points that represent cool and warm radiances of known value. Response of the radiometer is assumed to be linear between these extremes, which allows brightness temperatures to be assigned to radiances that fall between these extremes by linear interpolation.

The engineering method presented in NORDA Report 51 used 139 K for open water and 240 K for the high temperature, and applies only to the 1983 data set.

CONVERSION METHODS

The cool tie-point for both methods is represented by the radiometrically coolest surface observed in scenes of sea ice, open water at nadir. For our purposes, we have used 135 K. The warm tie-point is determined by using either a local ambient temperature, adjusted for the highest anticipated emissivity, or the reference load equivalent sensor temperature.

The first method discussed uses the ambient surface air temperature adjusted by the emissivity of first-year ice. Since eq 1 relates radiometric brightness temperature (T_b) in kelvins of a body with emissivity (E) to its physical temperature (T_t) in kelvins, and E ranges from 0.0 to 1.0, the radiometric temperature (T_b) of a substance should not exceed its physical temperature (T_t). The emissivity of any natural surface is less than 1.0, so the highest anticipated radiometric temperature in a scene is necessarily less than its physical temperature. Since first-year sea ice and some forms of young ice have the highest emissivity (0.94) of the objects scanned in these surveys, they will display the highest radiometric temperatures observed in KRMS images. We assume that the highest radiometric temperatures measured in a region correspond to areas of young first-year sea ice, and that the radiometric temperature of these surfaces is about 0.94 times the local physical temperature, expressed in kelvins.

The second method uses an internal reference load and equivalent sensor brightness temperature for the warm tie-point. There are three voltages measured at test points on the operator's console: B_1, B_0, and the reference load. B_1 is the level of the highest radiometer signal, B_0 is the level of the lowest radiometer signal, and the reference load is the voltage level to which the radiometer voltages are forcibly referenced. KRMS data are digitized across a 20-V range, with the highest signal level set at 10 V and the minimum at −10 V. Thus the B_1 value has to be scaled to 10 V by dividing $(B_1 - B_0)$ by 10, and then scaling the reference load by dividing it by the result of $(B_1 - B_0)/10$. Figure 1 is a graph produced at NWC by placing a thermocouple at the reference load and varying the reference load voltage and

Table 1. Comparison of sensor temperature with ambient and adjusted ambient temperature for KRMS missions flown between 1984 and 1988.

Date	*Sensor temp (K)*	*Ambient temp (K)*	*Adjusted ambient temp (K)*
1 July 1984	288		
3 July 1984	278		
21 March 1987	288	274	258
23 March 1987	276		
24 March 1987	280	272	256
26 March 1987	276	255	240
27 March 1987	273	257	
29 March 1987	273	257	
30 March 1987	273	257	
6 March 1988	273	257	
	274		
	279		
8 March 1988	280		
	291	273	257
	280	248	233
	278		
	276		
	276		
11 March 1988	279	276	259
	280		
	280		
	280		
	280		
	280		
	280	267	251
	280		
13 March 1988	279	259	243
	276		
	276		
	276	272	256
	276	272	256
	278		
	279	259	243
	279	259	243
14 March 1988	275		
	275		
	275		
	275		
	275		
	275		
	278		
	278		
	278		
	278		
	278		
	278		
	276		
	276	248	233

recording the resultant equivalent brightness temperature. Figure 2 illustrates the process used to obtain the reference load voltage used with the NWC graph to obtain the equivalent brightness temperatures for this study. When analog data are digitized, the gain and offset applied to the analog signal are adjusted such that the reference load voltage corresponds to a digital value of 0. By deriving the brightness temperature that is equivalent to the reference load and a digital value of 0, a warm tie-point is established. The cool tie-point, 135 K, is set at a digital value of 2000, and the data scaled linearly between these tie-points. The equivalent brightness temperature of the reference load has remained reasonably stable since 1984 and is always higher than the adjusted ambient temperature (Table 1).

Figure A1 provides both a comparison of the engineering conversion used for the 1983 data and the corresponding conversion graph computed using a local adjusted ambient temperature and open water. In this instance, they compare favorably. Examples of brightness temperature conversions obtained using both methods are shown as Figures A1-A17. The average slope of the conversion equation for the ambient temperature/open water method is 0.0584 with a standard deviation of 0.00549. The average slope for the sensor temperature/ open water method is 0.0728 with a standard deviation of 0.0027. The difference is several standard deviations (see Fig. A18). The ambient temperature method is greatly dependent on the accuracy, locality, and the timeliness of the measurement. The sensor (reference load equivalent) temperature has been very steady and is therefore recommended for use with existing data.

DIGITIZING

When the analog data are digitized, the 0 digital value is normally set equal to the reference load voltage. However, by observation, the lowest digital value corresponding to actual sea ice is usually higher than 0. Thus, the actual digital value for the highest brightness temperature should be determined for each set of data being converted and this value used for the warm tie-point.

CONCLUSIONS

Both methods evaluated produce brightness temperatures that appear to be reasonable for the types of surfaces being imaged. The sensor temperature method produces values that are approximately 20 K higher at the maxima; however, they compare reasonably well with observations from other radiometers. The cool tie-point (135 K) for open water is questionable and is a source of error in both methods. The actual digital value for the warm tie-point is another questionable point and will vary between data sets.

The ambient temperature method is predicated on the availability of timely and accurate surface measurements of physical temperature and the validity of the assumption that the highest brightness temperature in a scene is less than the measured ambient. This method is based on surface datum and does not require that corrections be made for atmospheric contributions.

The sensor temperature method appears to be the more repeatable method. It produces brightness temperatures that appear to be reasonable when compared with the March 1983 data and other sources (such as surface-based measurements and airborne Advanced Multichannel Microwave Radiometer data). This method is affected by the atmospheric contributions, as the warm tie-point is internal to the sensor. The cool tie-point (water) is a surface measurement. Atmospheric models exist that may provide some value of correction for the brightness temperatures derived using the sensor temperature and open water method. The derived values presented in this report are few in number and are therefore insufficient to form a final conclusion as to the accuracy of this method and recommended for relative comparisons only.

This investigation has not resulted in any method that consistently and reliably produces calibrated brightness temperatures and only serves to emphasize the need for the addition of real-time calibration sources to the KRMS sensor.

REFERENCES

Eppler, D.T., L.D. Farmer, A.W. Lohanick and M. Hoover (1984) Digital processing of passive K_a-band microwave images for sea ice classification. Naval Ocean Research and Development Activity, Stennis Space Center, Mississippi, NORDA Report 51.

Eppler, D.T., L.D. Farmer, A.W. Lohanick and M. Hoover (1986) Classification of sea ice types with single band (33.6-GHz) airborne passive microwave imagery. *Journal of Geophysical Research*, **91**(C9): 10,661–10,695.

Farmer, L.D., D.T. Eppler, B. Heydlauff and D.A. Olsen (1989) KRMS GEOSAT/LIMEX 87 Quick Look report. Naval Ocean Research and Development Activity, Hanover, New Hampshire, NORDA Technical Note 385.

Hollinger, J.P. (1973) Microwave properties of a calm sea. Naval Research Laboratory, Washington, D.C., NRL Report 7110-2.

Hollinger, J.P. and R.C. Lo (1983) SSM/I project summary report. Naval Research Laboratory, Washington, D.C., NRL Memorandum Report 5055.

Stogryn, A. (1971) Equations for calculating the dielectric constant of saline water. Institute of Electrical and Electronics Engineers, *Transactions on Microwave Theory and Techniques*, **MTT-19**: 733–735.

APPENDIX A: BRIGHTNESS TEMPERATURE CONVERSION CHARTS

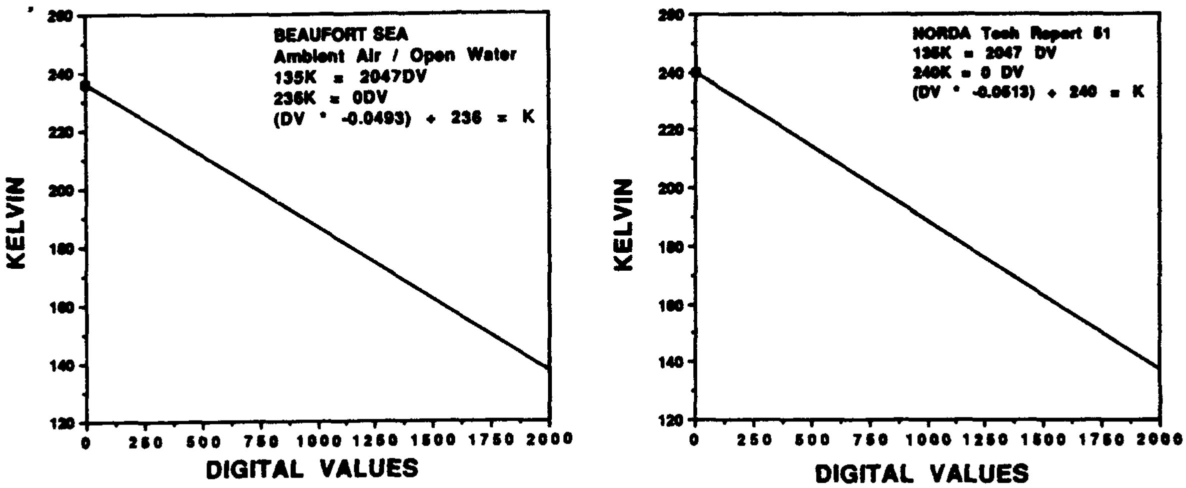

Figure A1. Brightness temperature conversion chart for March 1983.

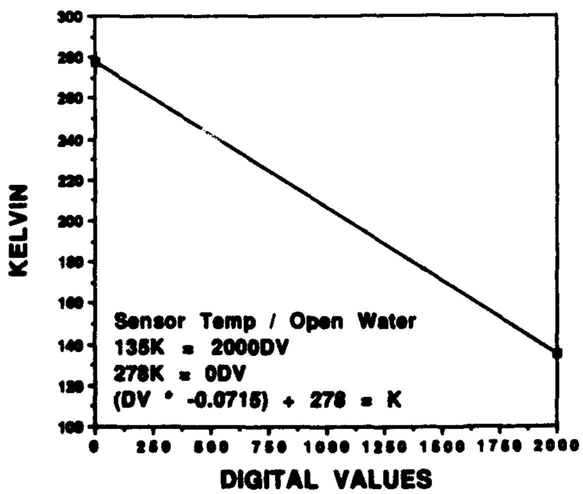

Figure A2. Brightness temperature conversion chart for 3 July 1984.

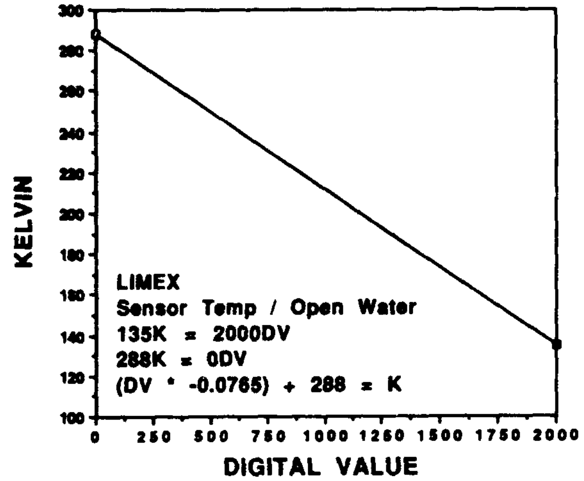

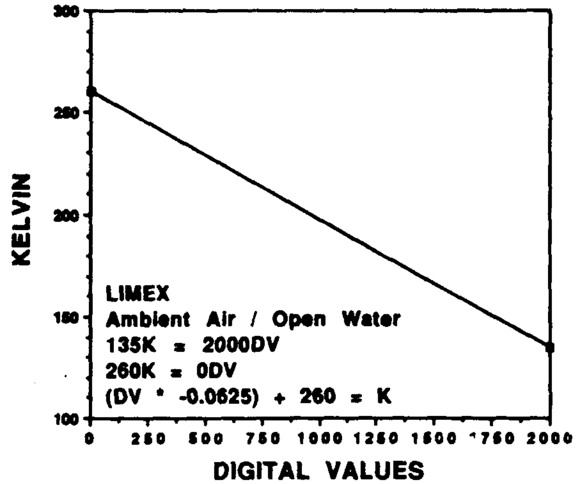

Figure A3. Brightness temperature conversion chart for 21 March 1987.

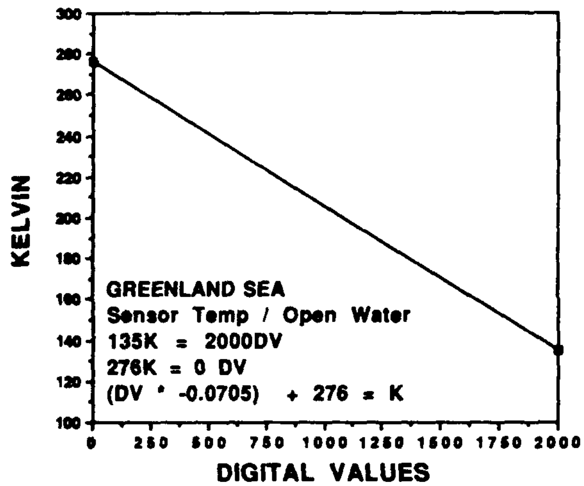

Figure A4. Brightness temperature conversion chart for 23 and 26 March 1987.

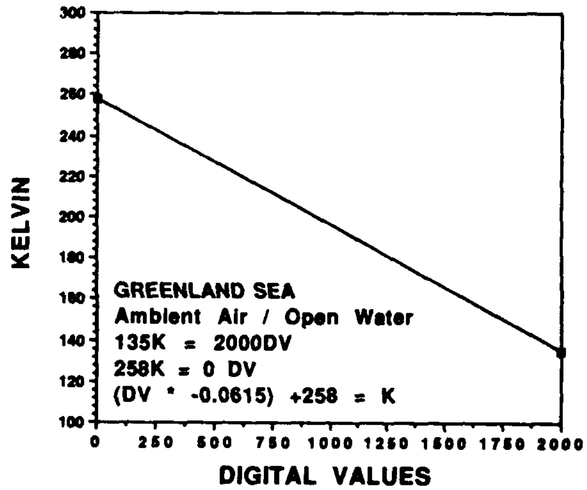

Figure A5. Brightness temperature conversion chart for 24 March 1987.

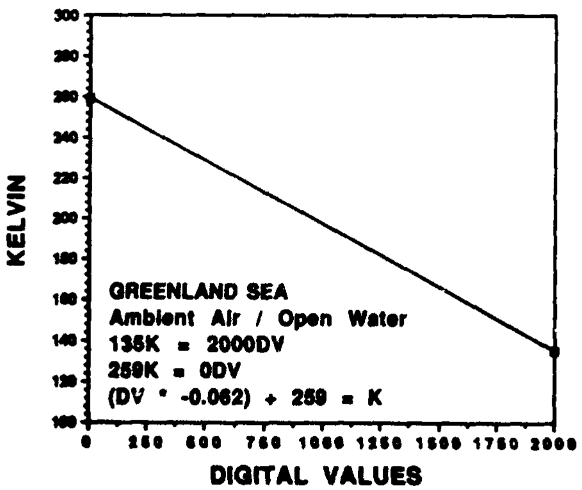

Figure A6. Brightness temperature conversion chart for 27 and 29 March 1987.

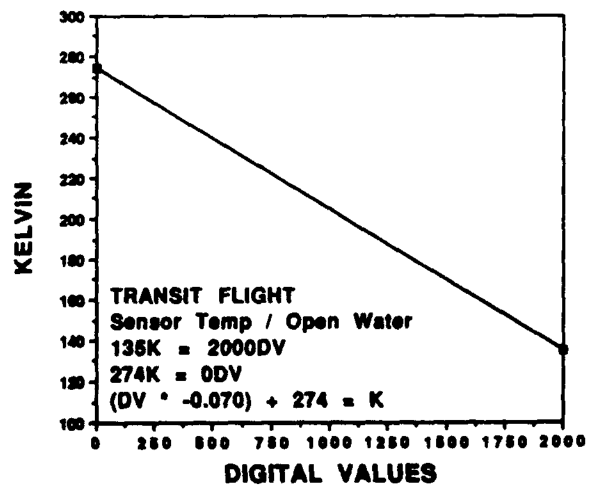

Figure A7. Brightness temperature conversion chart for 6 March 1988.

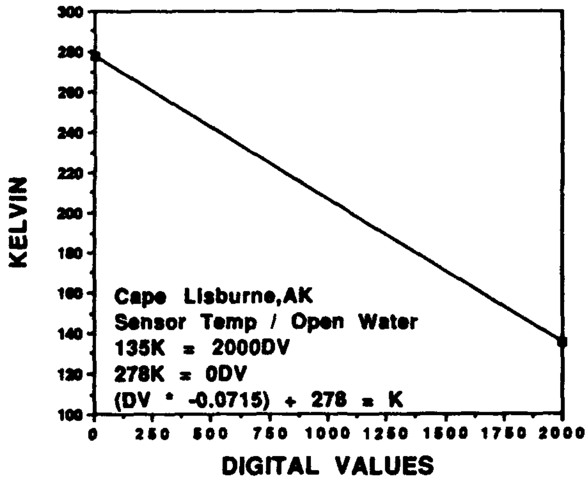

Figure A8. Brightness temperature conversion chart for 8 March 1988, Cape Lisburne, Alaska.

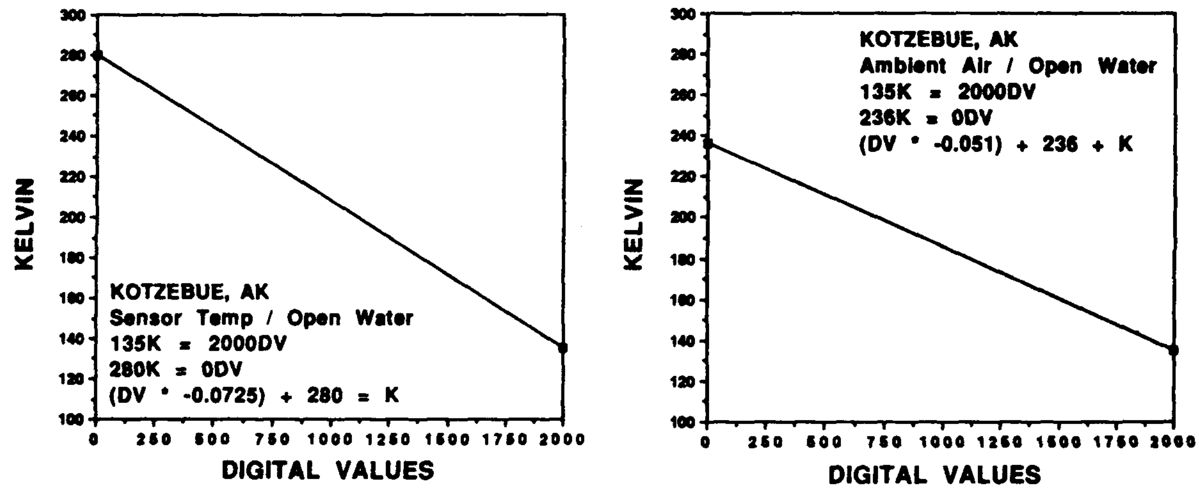

Figure A9. Brightness temperature conversion chart for 8 March 1988, Kotzebue, Alaska.

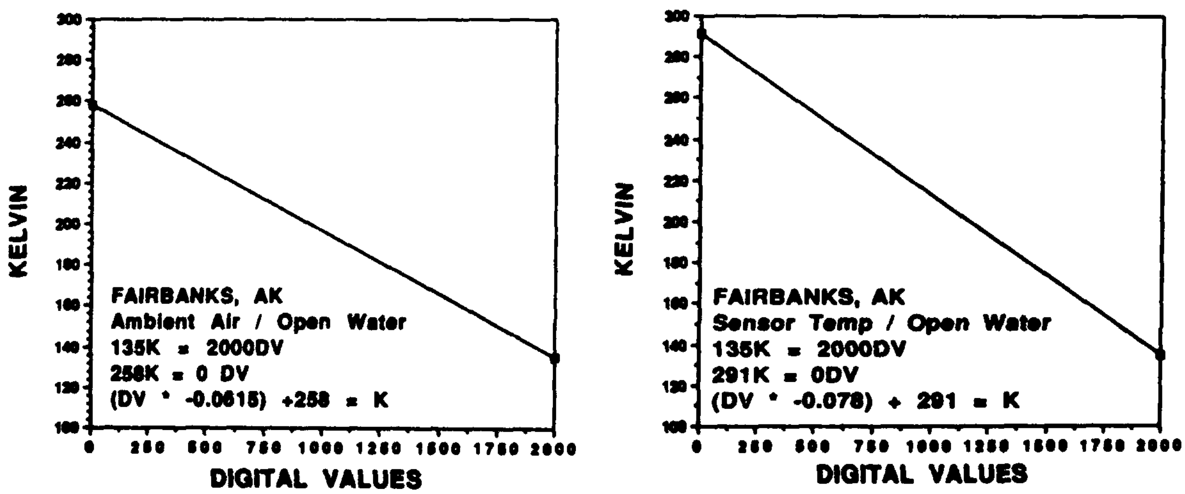

Figure A10. Brightness temperature conversion chart for 8 March 1988, Fairbanks, Alaska.

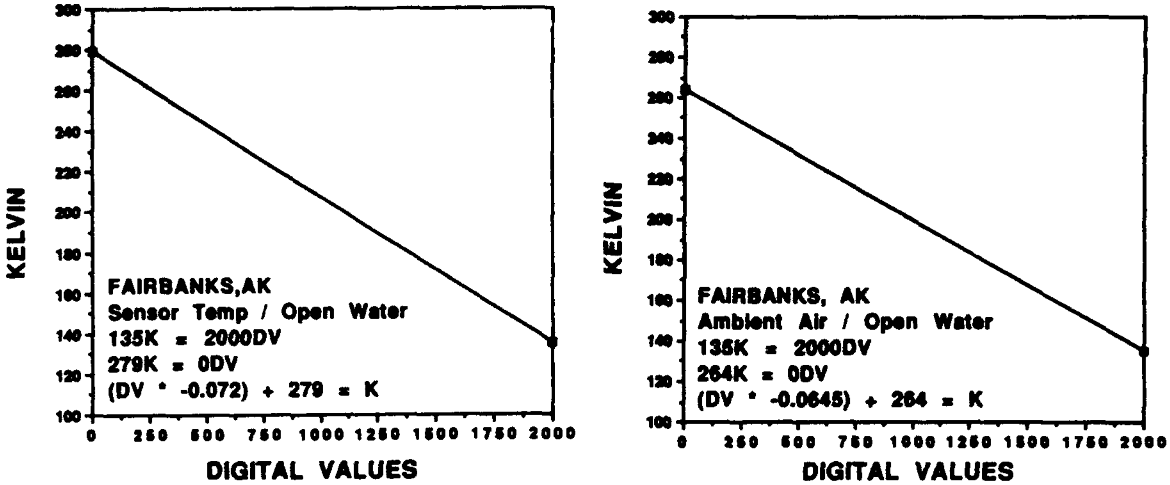

Figure A11. Brightness temperature conversion chart for 11 March 1988, Fairbanks, Alaska.

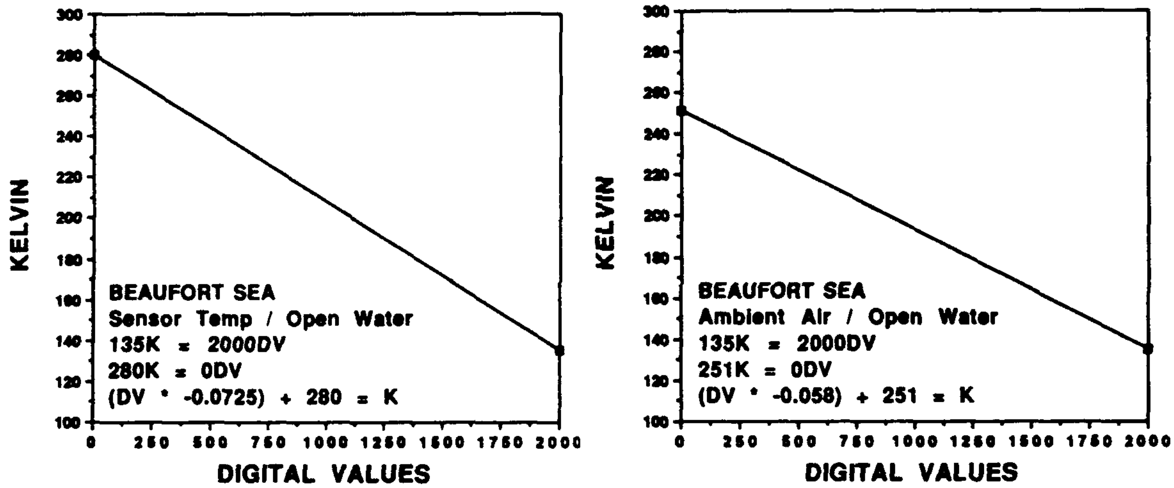

Figure A12. Brightness temperature conversion chart for 11 March 1988, Beaufort Sea.

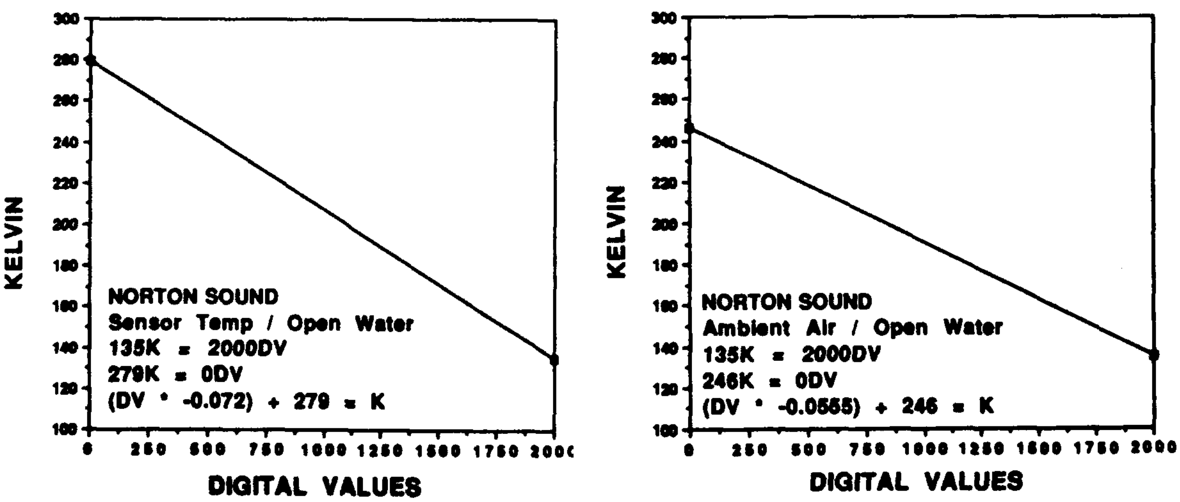

Figure A13. Brightness temperature conversion chart for 13 March 1988, Norton Sound.

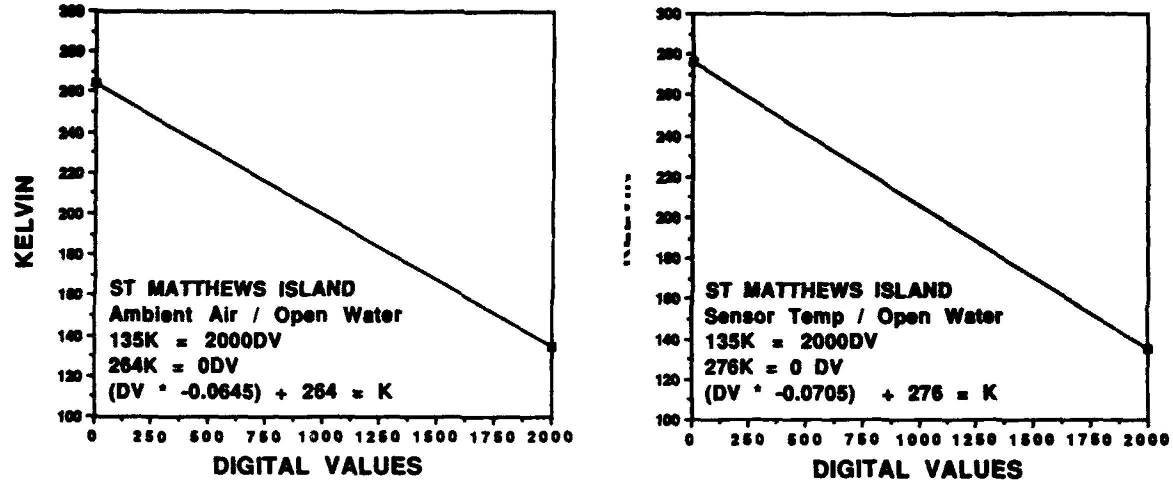

Figure A14. Brightness temperature conversion chart for 13 March 1988, St. Matthews Island.

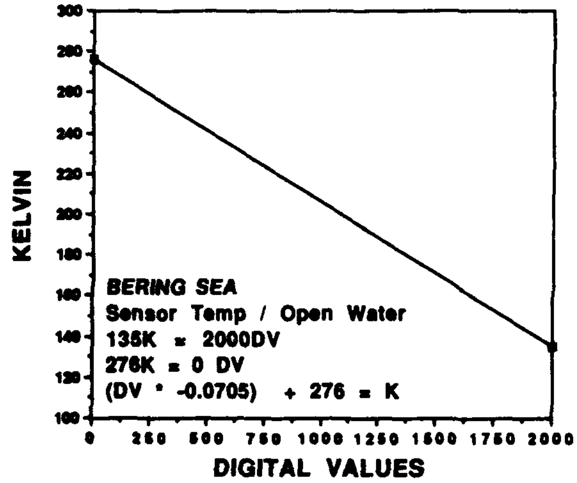

Figure A15. Brightness temperature conversion chart for 13 March 1988, Bering Sea.

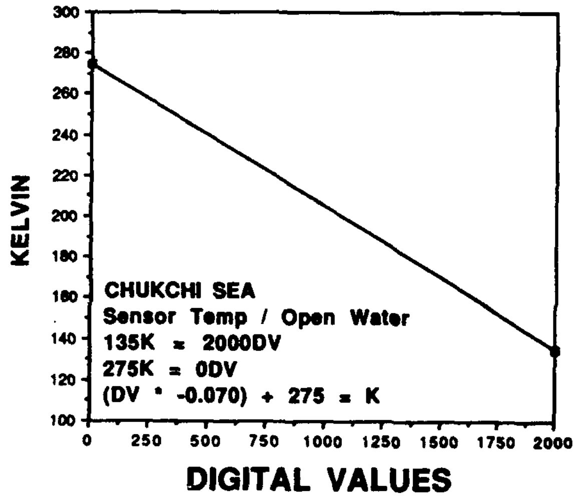

Figure A16. Brightness temperature conversion chart for 14 March 1988, Chukchi Sea.

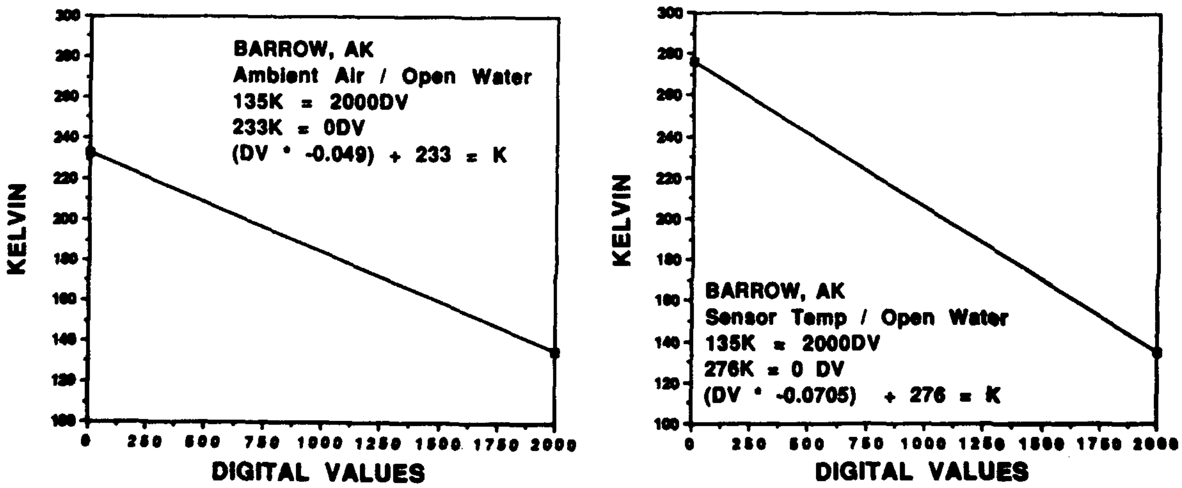

Figure A17. Brightness temperature conversion chart for 14 March 1988, Barrow, Alaska.

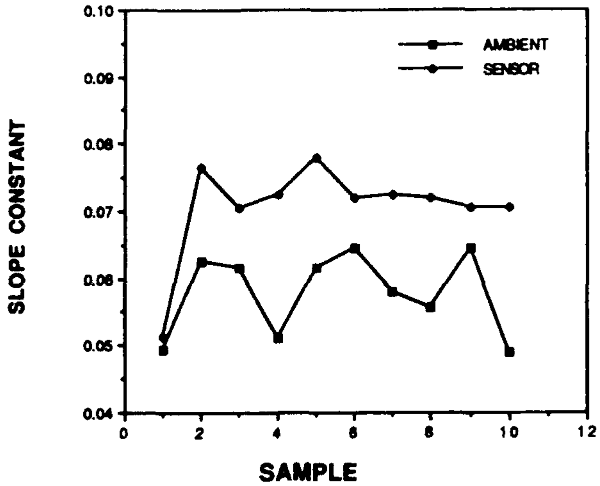

Figure A18. Conversion constant comparison.

APPENDIX B: DISTRIBUTION LIST

Dr. Lyn Arsenault
Cold Regions Remote Sensing
Box 526
Sittsville, Ontario K2S 1A6, Canada

Mr. David Benner
Naval Polar Oceanography Center
4301 Suitland Road
Suitland, Maryland 20390

Dr. Frank Carsey
Jet Propulsion Laboratory
4800 Oak Grove Drive
Pasadena, California 91109

Dr. Donald Cavalieri
Laboratory for Oceans
Code 671
NASA Goddard Space Flight Center
Greenbelt, Maryland 20771

Ms. Nita Chase
NOARL Code 321
Stennis Space Center, Mississippi 39529-5004

Mr. Michael Collins
Institute for Space and Terrestrial Science
48 Nassau Street
Toronto, Ontario M5T 1M2, Canada

Dr. Josefino Comiso
Laboratory for Oceans
Code 671
NASA Goddard Space Flight Center
Greenbelt, Maryland 20771

Mr. John Crawford
Jet Propulsion Laboratory
4800 Oak Grove Drive
Pasadena, California 91109

Dr. Thomas Curtin
Code 1125AR
Office of Naval Research
800 North Quincy St.
Arlington, Virginia 22217

Mr. Mark Drinkwater
Jet Propulsion Laboratory
4800 Oak Grove Drive
Pasadena, California 91109

Mr. Robert Fett
NOARL Code 441
Monterey, California 93943-5006

Ms. Florence Fetterer
NOARL Code 321
Stennis Space Center, Mississippi 39529-5004

Dr. William Full
FIMTSI
Department of Geology
The Wichita State University
Wichita, Kansas 67208

Mr. Larry Gatto
USACRREL
72 Lyme Road
Hanover, New Hampshire 03755-1290

Dr. Albert Green
NOARL Code 330
Stennis Space Center, Mississippi 39529-5004

Dr. Thomas Grenfell
Department of Atmospheric Science
AK-40
University of Washington
Seattle, Washington 98195

Mr. Jeffrey Hawkins
NOARL Code 321
Stennis Space Center, Mississippi 39529-5004

Mr. Richard Hays
Office of the Oceanographer of the Navy
U.S. Naval Observatory
34th and Massachusetts Ave. NW
Washington, D.C. 20392-1800

Dr. Frank Herr
Code 1121RS
Office of Naval Research
800 North Quincy St.
Arlington, Virginia 22217

Mr. Bruce Heydlauff
Code 3521
Naval Weapons Center
China Lake, California 93555

Dr. James Hollinger
Naval Research Laboratory
4555 Overlook Ave., SW
Washington, D.C. 20375

Dr. Ronald Holyer
NOARL Code 321
Stennis Space Center, Mississippi 39529-5004

Mr. Mervyn Hoover
TRW
1 Rancho Carmel
RC7/1417
San Diego, California 92128

Dr. Ken Jezek
Byrd Polar Science Center
The Ohio State University
125 South Oval Mall
Columbus, Ohio 43210

Dr. Thomas Kinder
Code 1122ML
Office of Naval Research
800 North Quincy St.
Arlington, Virginia 22217

Mr. Austin Kovacs
USACRREL
72 Lyme Road
Hanover, New Hampshire 03755-1290

Dr. Ron Kwok
Jet Propulsion Laboratory
4800 Oak Grove Drive
Pasadena, California 91109

Mr. Seymour Laxon
University College/London
Mollard Space Science Laboratory
Holmbury St. Mary
Dorking, Surrey RH5 6N7, United Kingdom

Dr. Lewis Link
USACRREL
72 Lyme Road
Hanover, New Hampshire 03755-1290

Dr. Chuck Livingstone
Canada Center for Remote Sensing
2464 Sheffield Road
Ottawa, Ontario K1A OY7, Canada

Mr. Charles Luther
Code 1121RS
Office of Naval Research
800 North Quincy St.
Arlington, Virginia 22217

Dr. Seelye Martin
School of Oceanography
WB-10
University of Washington
Seattle, Washington 98195

Dr. Harlan McKim
USACRREL
72 Lyme Road
Hanover, New Hampshire 03755-1290

Dr. Lyn McNutt
RADARSAT Project Office
Canadian Space Agency
Suite 200
110 O'Connor St.
Ottawa, Ontario K1A 1A1, Canada

Ms. Rae Melloh
USACRREL
72 Lyme Road
Hanover, New Hampshire 03755-1290

Dr. Donald Montgomery
Department of the Navy
Space and Naval Warfare Systems Command
PMW-141
Building NC-1, Room 3E90
Washington, D.C. 20363-5100

Dr. Richard K. Moore
Radar Systems and Remote Sensing Laboratory
University of Kansas
2291 Irving Hill Road
Lawrence, Kansas 66045-2969

Mr. George Newton
Analysis and Technology Corporation
Two Crystal Park, 8th Floor
2121 Crystal Drive
Arlington, Virginia 22202

Dr. Vince Noble
Code 8310
Naval Research Laboratory
4555 Overlook Ave., SW
Washington, D.C. 20375

Prof. Nubuo Ono
Institute of Low Temperature Science
Hokkaido University
Kita-19, Nishi-8, Kita-ku, Sapporo 060, Japan

Dr. Robert Onstott
ERIM
P.O. Box 8618
Ann Arbor, Michigan 48107-8618

Mr. Steve Payne
NOARL Code 440
Monterey, California 93943-5006

Dr. Carol Pease
NOAA/PMEL
7600 Sand Point Way NE
Seattle, Washington 98115

Dr. Jay Perlman
TRW
R1-1078
1 Space Park
Redondo Beach, California 90278

Dr. Ruth Preller
NOARL Code 322
Stennis Space Center, Mississippi 39529-5004

Mr. Charles Radl
Naval Underwater Systems Center
Newport, Rhode Island 02841

Dr. Rene Ramseier
Institute for Space and Terrestrial Science
48 Nassau Street
Toronto, Ontario M5T 1M2, Canada

Dr. Eric Rignot
Jet Propulsion Laboratory
4800 Oak Grove Drive
Pasadena, California 91109

Mr. Quincy Robe
Coast Guard Research and Development Center
OCB Branch
Avery Point
Groton, Connecticut 06340-6096

Dr. Drew Rothrock
Applied Physics Laboratory
University of Washington
1013 NE 40th St.
Seattle, Washington 98105

Dr. Irene Rubinstein
Institute for Space and Terrestrial Science
48 Nassau Street
Toronto, Ontario M5T 1M2, Canada

Ms. Karen St. Germain
MIRSL
Dept. of Electrical and Computer Engineering
University of Massachusetts
Amherst, Massachusetts 01003

Dr. Axel Schweiger
CIRES
University of Colorado
Campus Box 449
Boulder, Colorado 80309

Dr. Kunio Shirasawa
Sea Ice Research Laboratory
Hokkaido University
Minamigaoka 6-4-10
Monbetsu 094, Japan

Dr. William Stringer
Geophysical Institute
University of Alaska
Fairbanks, Alaska 99701

Dr. Robert Shuchman
ERIM
P.O. Box 8618
Ann Arbor, Michigan 48107-8618

Dr. Konrad Steffen
CIRES
University of Colorado
Campus Box 449
Boulder, Colorado 80309

Dr. James Street
Department of Geology
St. Lawrence University
Canton, New York 13617

Dr. Calvin Swift
MIRSL
Dept. of Electrical and Computer Engineering
University of Massachusetts
Amherst, Massachusetts 01003

Dr. Robert Thomas
Code EEC
NASA Headquarters
Washington, D.C. 20546

Mr. Walter B. Tucker
USACRREL
72 Lyme Road
Hanover, New Hampshire 03755-1290

Dr. Lars Ulander
Canada Center for Remote Sensing
2464 Sheffield Road
Ottawa, Ontario K1A OY7, Canada

Dr. Wilford Weeks
Geophysical Institute
University of Alaska
Fairbanks, Alaska 99701

Dr. Pat Welsh
USACRREL
72 Lyme Road
Hanover, New Hampshire 03755-1290

Dr. Dale Winebrenner
Applied Physics Laboratory
University of Washington
1013 NE 40th St.
Seattle, Washington 98105

Mr. Gary Wohl
Naval Polar Oceanography Center
4301 Suitland Road
Suitland, Maryland 20390

Dr. Ronald Woodfin
Division 333
Sandia National Laboratories
Albuquerque, New Mexico 87185

REPORT DOCUMENTATION PAGE

Form Approved
OMB No. 0704-0188

1. AGENCY USE ONLY (Leave blank)	2. REPORT DATE	3. REPORT TYPE AND DATES COVERED
	September 1990	March 1983 to March 1988

4. TITLE AND SUBTITLE

Converting Digital Passive Microwave Radiances to Kelvin Units of Brightness Temperatures

5. FUNDING NUMBERS

PE: 990101/61153N
PR: 00101/3205
TA: 0/330
WU: DN258060/DN256025

6. AUTHORS

L. Dennis Farmer, Duane T. Eppler and Alan W. Lohanick

7. PERFORMING ORGANIZATION NAME(S) AND ADDRESS(ES)

Naval Oceanographic and Atmospheric Research Laboratory*
Polar Oceanography Branch
Hanover, New Hampshire 03755-1290

8. PERFORMING ORGANIZATION REPORT NUMBER

NORDA Technical Note 427

9. SPONSORING/MONITORING AGENCY NAME(S) AND ADDRESS(ES)

Naval Oceanographic and Atmospheric Research Laboratory*
Ocean Science Directorate
Stennis Space Center, Mississippi 39529-5004

10. SPONSORING/MONITORING AGENCY REPORT NUMBER

NORDA Technical Note 427

11. SUPPLEMENTARY NOTES

* Formerly Naval Ocean Research and Development Activity

12a. DISTRIBUTION/AVAILABILITY STATEMENT

Approved for public release; distribution is unlimited.

12b. DISTRIBUTION CODE

13. ABSTRACT (*Maximum 200 words*)

The K_a-band Radiometric Mapping System (KRMS) has been utilized since 1983 to collect digital records of microwave radiances. This report details methods for converting these digital radiances to appropriate units of brightness temperature.

14. SUBJECT TERMS

Brightness temperature, **Digital radiances**, **KRMS**, **Passive microwave**, **Sea ice**

15. NUMBER OF PAGES 19

16. PRICE CODE

17. SECURITY CLASSIFICATION OF REPORT	18. SECURITY CLASSIFICATION OF THIS PAGE	19. SECURITY CLASSIFICATION OF ABSTRACT	20. LIMITATION OF ABSTRACT
UNCLASSIFIED	UNCLASSIFIED	UNCLASSIFIED	SAR

NSN 7540-01-280-5500

Standard Form 298 (Rev. 2-89)
Prescribed by ANSI Std. Z39-18
298-102